XI International Conference on Computational Methods for Coupled Problems in Science and Engineering
COUPLED PROBLEMS 2025
A. Larese, S. Perotto and G. Rozza (Eds)

A FEM-FVM COUPLING CODE FOR NUMERICAL SIMULATION OF A LIQUID METAL HEAT EXCHANGER

S. BALDINI[1], G. BARBI[2], A. CERVONE[1], F. GIANGOLINI[1], V. LA SALANDRA[3], S. MANSERVISI[1], L. SIROTTI[*,1]

[1] Department of Industrial Engineering (DIN)
Alma Mater Studiorum - Università di Bologna
Lab. of Montecuccolino, 40136 Bologna, Italy
e-mail: lucia.sirotti4@unibo.it, web page: https://ingegneriaindustriale.unibo.it/it

[2] Department of Mathematics and Statistics,
Texas Tech University,
Lubbock, Texas, USA

[3] Systems Engineering Area,
NIER Ingegneria S.p.A.,
Via C. Bonazzi 2, 40013 Castel Maggiore, Bologna, Italy

Key words: Code Coupling, Heat Exchanger, Conjugate Heat Transfer, MEDCoupling Library

Abstract. Over the past few years, multiscale and multiphysics problems have drawn significant attention from the scientific community. Simulating these complex phenomena requires the integration of multiple physics domains which raises significant challenges for computational tools, as most existing codes are designed to address specific problem types. Two primary strategies have emerged over the years: the monolithic approach, which develops a unified numerical code to model all relevant phenomena, and the coupling of existing validated codes to leverage their strengths and peculiarities.

This paper presents a numerical code coupling technique that integrates modules from various Computational Fluid Dynamics (CFD) codes into a unified numerical platform, enabling the simulation of coupled multiphysics and multiscale problems. The coupling strategy presented in this work involves the data transfer between the in-house finite element method (FEM) code, FEMuS, and the finite volume method (FVM) code, OpenFOAM. The integration between the CFD codes is performed using the MEDCoupling library, which provides algorithms for efficient in-memory communication.

In this work, the numerical coupling application is presented by simulating a Conjugate Heat Transfer problem that thermally couples solid and fluid domains. In particular, the boundary data transfer algorithm is applied to a realistic case of a PbLi-air heat exchanger. Within the fluid domain, the liquid metal turbulent flow is simulated using the FEMuS solver, which employs an anisotropic four-parameter turbulence model specifically designed for low-Prandtl-number fluids. The fluid domain is numerically coupled through the physical fluid-solid interface with the solid one, where OpenFOAM handles the tube energy equation and the fins-air interaction.

1 INTRODUCTION

In recent years, the study of multiscale and multiphysics problems has become a major research focus. Multiscale modeling simulates processes at different spatial and temporal scales, while multiphysics modeling couples distinct physical models to capture interactions between phenomena. Examples include nuclear reactor plants, where neutronics, thermohydraulics, and thermomechanics are strongly coupled, or heat exchangers, where Conjugate Heat Transfer (CHT) links fluid dynamics with solid heat conduction. In this context, the integration of High-Performance Computing (HPC) with CFD enables large-scale simulations of complex multiscale and multiphysics systems with high fidelity.

Two main strategies exist for multiphysics and multiscale simulation: monolithic approaches solve all phenomena simultaneously in a single code, yielding highly accurate and stable solutions but requiring complex formulations and specialized solvers. Partitioned approaches couple existing solvers, solving each subsystem independently and exchanging data between them. This method reuses validated codes, supports parallel execution, and improves flexibility, but requires efficient in-memory data transfer to avoid file I/O bottlenecks.

This work focuses on developing a coupling application to enable data transfer between FVM and FEM solvers at the interface of two physical domains. In the context of heat transfer, these interfaces are classified as conjugate problems, where the so-called conjugate boundary condition can be applied. This coupling application enhances an in-house numerical platform for multiphysics and multiscale simulations. The platform uses both FEM and FVM to model fluids and solids [2], integrating OpenFOAM [1] with the FEMuS library [3] to combine their strengths. In this work, the FEMuS and OpenFOAM codes have been coupled into the numerical platform using the MED library [4] as a common intermediate representation for exchanging heterogeneous data structures [11].

2 HEAT EXCHANGER DESCRIPTION

This work investigates numerical strategies for simulating a realistic PbLi–air heat exchanger designed by the Italian company Nier Ingegneria S.p.A., using the developed coupling application and interface-coupling approach described in [11].

The analyzed heat exchanger is part of the International Thermonuclear Experimental Reactor (ITER) Test Blanket Modules (TBMs) program, which aims to validate tritium breeding concepts and heat extraction technologies for future fusion power plants. Results from the TBM campaign will directly inform the design of DEMO, the demonstration fusion power plant that will follow ITER [5]. TBMs require multiple ancillary systems for operation, monitoring, and integration within ITER. These include cooling loops, tritium extraction systems, neutron diagnostics, and safety systems [6]. Among them, the Lead–Lithium (PbLi) loop plays a key role in some TBMs, serving both as the breeder material (producing tritium via neutron–lithium reactions) and as the primary coolant.

Under normal operation, the PbLi returns from the TBM at approximately $673\,\mathrm{K}$, with a mass flow rate in the range of 0.2–$1.0\,\mathrm{kg/s}$. The alloy is then heated to $723\,\mathrm{K}$ and fed into the Tritium Extraction Unit (TEU), which removes tritium into the gas phase. Downstream, a heat exchanger cools the PbLi to about $573\,\mathrm{K}$ using a dual cooling system: a closed air circuit (primary coolant) and a water circuit connected to ITER's Component Cooling Water System (CCWS). A portion of the cooled PbLi then flows through a cold trap (CT) for alloy purification,

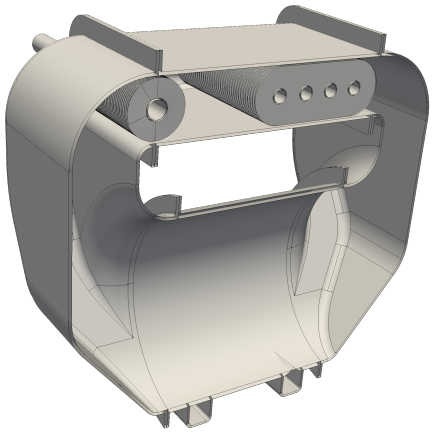

Figure 1: Geometry of the PbLi loop cooler.

while the rest is directed to the storage/drain tank.

Figure 1 shows the PbLi loop heat exchanger model. The system comprises an outer casing that guides airflow from a fan located in the lower chamber to the upper section, which houses the tube bundle. The air first passes through the tube bundle, extracting heat from the PbLi, and then through a cooling coil, where it is further cooled by the water circuit.

This cooling system must ensure that the PbLi flow meets the TBM inlet temperature requirement while staying safely above the alloy's freezing point. The coldest point in the loop is not the heat exchanger outlet but the CT outlet pipe, where PbLi reaches $526\,\mathrm{K}$, approximately $16\,\mathrm{K}$ above its freezing temperature [7]. If needed, heating cables prevent further temperature drops. Consequently, the analysis of heat exchanger performance focuses on meeting the upper temperature limit at the TBM inlet, while lower temperatures are acceptable as long as they remain above the solidification threshold.

2.1 Constraints and properties of the PbLi-air heat exchanger

In this study, the performance assessment focuses only on the critical section of the heat exchanger in Figure 1, the PbLi-air heat exchanger. According to the constraints, the cooler system of the PbLi loop is designed to reduce the temperature of the PbLi alloy flow from $723\,\mathrm{K}$ to $573\,\mathrm{K}$, achieving a temperature reduction of $150\,\mathrm{K}$. The mass flow rate of the liquid metal is set at $0.63\,\mathrm{kg/s}$, corresponding to the thermal power extraction of $17870\,\mathrm{W}$. This cooling is accomplished using an airflow that externally sweeps the pipe with a mass flow rate of $1.517\,\mathrm{kg/s}$. The air temperature is set to $333\,\mathrm{K}$, and it absorbs the heat from the liquid metal as it flows through the tube. As seen in Figure 1, the PbLi-air heat exchanger consists of a single pipe with a hydraulic diameter of $D_h = 0.03\,\mathrm{m}$ and a length of $L = 0.6\,\mathrm{m}$. The pipe is made of EUROFER (EUROpean FERritic-martensitic steel) [8] with a thickness of $0.004\,\mathrm{m}$ and is covered by 120 copper fins, each with an average length of $0.014\,\mathrm{m}$.

Table 1 reports the physical properties of the materials used in the following simulations. In particular, the properties of the liquid metal refer to the Pb-rich eutectic alloy Pb-16Li (16 at.% Li) at the operational temperature of $648\,\mathrm{K}$ [7]. EUROFER is a low-carbon ferritic-martensitic steel optimized for resistance to neutron irradiation damage [8]. Its thermophysical properties

Table 1: Physical properties of the involved materials.

Material	$\rho\,[\frac{\text{kg}}{\text{m}^3}]$	$\lambda\,[\frac{\text{W}}{\text{mK}}]$	$c\,[\frac{\text{J}}{\text{kgK}}]$	μ [Pa s]
PbLi	9749	21.9	189.1	0.0017
Air	1.225	0.0292	1008.2	0.00002
EUROFER	7798	28.8	512.70	-
Copper	8933	401	385	-

are reported at temperatures corresponding to the operating temperature of the liquid metal.

3 LEAD-LITHIUM SIMULATION

First, we performed simulations of the turbulent flow of the lead–lithium (PbLi) alloy inside the EUROFER tube to assess and compare the performance of the turbulent models implemented in the two CFD codes, FEMuS and OpenFOAM. Thus, the PbLi flow was initially simulated using the monolithic turbulent solvers available in both FEMuS and OpenFOAM, providing a consistent basis for evaluating their accuracy and capabilities. Exploiting the symmetry of the problem, the computational domain is simplified. The PbLi flow is simulated over the whole pipe length, using an axisymmetric configuration in FEMuS and a wedge configuration in OpenFOAM. The geometry is illustrated in Figure 2. For FEMuS, the domain is reduced

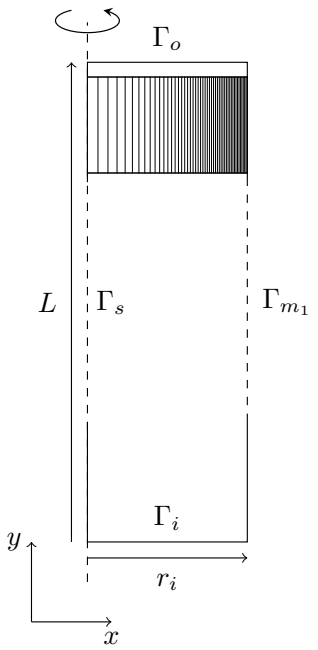

Figure 2: Schematic representation of the computational domain for Lead-Lithium flow simulation.

to a 2D rectangle with a base of $r_i = 0.015$, m and length $L = 0.6$, m. OpenFOAM employs an equivalent wedge geometry with the same radius and length. Both meshes are refined near the wall to ensure $y^+ < 1$, with the first cell adjacent to the wall having a thickness of 1×10^{-4}, m.

The resulting computational grid consists of 14792 cells, with 172 cells along the y-direction and 86 along the radial direction for both simulations.

Given the operational temperature range, thermal variations of the PbLi properties are considered negligible. The flow is fully forced, and buoyancy effects are neglected in the governing equations. In particular, FEMuS solves the following RANS system of equations

$$\frac{\partial \langle u_i \rangle}{\partial x_i} = 0\,, \tag{1}$$

$$\frac{D\langle u_i \rangle}{Dt} = -\frac{1}{\rho}\frac{\partial \langle p \rangle}{\partial x_i} + \frac{\partial}{\partial x_j}\left[\nu\left(\frac{\partial \langle u_i \rangle}{\partial x_j} + \frac{\partial \langle u_j \rangle}{\partial x_i}\right) - \langle u_i' u_j' \rangle\right]\,, \tag{2}$$

$$\frac{D\langle T \rangle}{Dt} = \frac{\partial}{\partial x_i}\left(\alpha \frac{\partial \langle T \rangle}{\partial x_i} - \langle u_i' T' \rangle\right)\,. \tag{3}$$

The Reynolds stress tensor and turbulent heat flux are computed using the Explicit Algebraic Stress Model (EASM) and Explicit Algebraic Heat-Flux Model (EAHFM) described in [9]. These models provide the expressions for $\langle \mathbf{u}'\mathbf{u}' \rangle$ and $\langle \mathbf{u}' T' \rangle$, as detailed in [11]. Model closure is achieved through the logarithmic four-parameter turbulence model $K - \Omega - K_\theta - \Omega_\theta$ [10].

OpenFOAM, instead, solves for the RANS system of equations (1)-(3) using the Boussinesq hypothesis. The turbulent viscosity is computed with the `kOmegaSST` model, while the turbulent diffusivity is derived through the Reynolds analogy with $Pr_t = 0.85$.

The simulation assumes that the lead–lithium alloy reaches a fully developed velocity profile before entering the heat exchanger, while the thermal field is modeled as developing, reflecting the realistic condition where the flow enters at its maximum temperature and cools progressively along the pipe. For the velocity field, both FEMuS and OpenFOAM impose a no-slip condition on the pipe wall, Γ_w. In FEMuS, fully developed flow is achieved by imposing pressure values at the inlet and outlet (Γ_i and Γ_o), which generate the pressure drop required to obtain the target mass flow rate. OpenFOAM, on the other hand, employs mapped boundary conditions between the inlet and outlet and enforces a fully developed regime by applying a `meanVelocityForce` constraint, fixing the bulk velocity to 0.0914, m/s. Symmetry is imposed along the rotation axis through a homogeneous Neumann condition in FEMuS, while OpenFOAM applies a `wedge` boundary condition on the front and back faces of the wedge geometry.

The thermal field is initialized by setting the inlet temperature to a uniform 723, K, representing the maximum PbLi temperature. A homogeneous wall heat flux of $\dot{q} = -315998, \mathrm{W/m^2}$ is imposed on Γ_w, corresponding to the design thermal load, while a homogeneous Neumann condition is applied at the outlet. Symmetry conditions are applied to the remaining surfaces.

Turbulent quantities are treated consistently with the RANS closure models. FEMuS applies zero-gradient conditions for k, ω, k_θ and ω_θ at the inlet and outlet, and imposes the near-wall conditions described in [10] on Γ_w. OpenFOAM uses mapped boundary conditions at inlet and outlet and applies the built-in `kqRWallFunction` and `omegaWallFunction` on Γ_w for k and ω, respectively.

3.1 Numerical results and DNS comparison

This section provides a detailed analysis of the results from the dynamic fields. Since the flow is fully developed, its dynamic behavior can be examined independently of the thermal

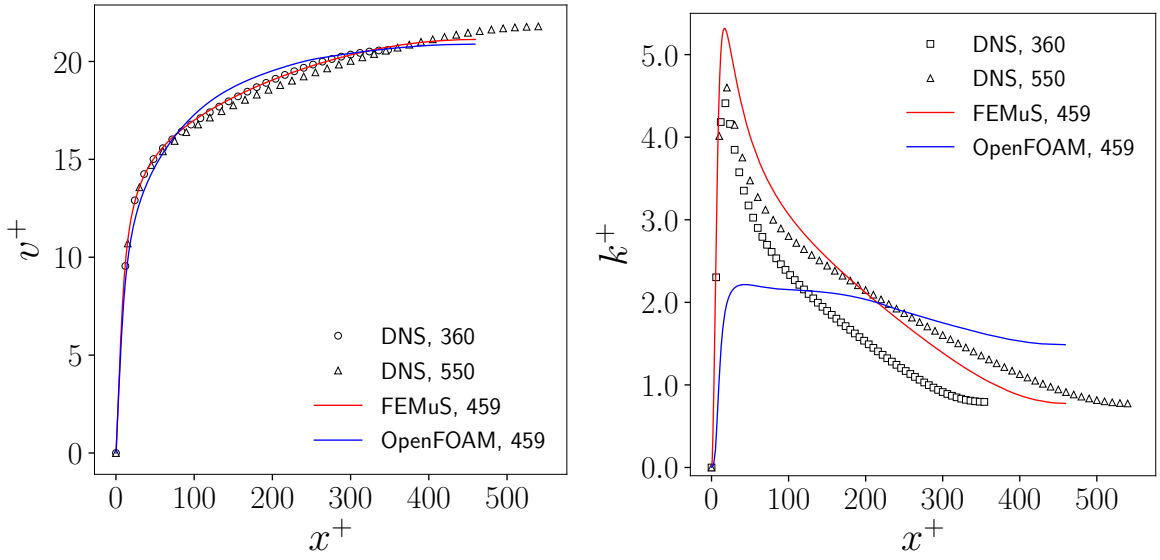

Figure 3: Comparison between DNS dataset ($Re_\tau = 360$ and $Re_\tau = 550$) from [12] and the heat exchanger results (corresponding to the case of $Re_\tau = 459$). Non-dimensional velocity profiles on the left and turbulent kinetic energy profiles on the right.

field. The forced-convection regime ensures that the developing temperature profile does not affect the velocity distribution, allowing a direct and meaningful comparison with DNS results from the literature. Several DNS reference databases are available for pipe flows at different friction Reynolds numbers, $Re_\tau = u_\tau \delta / \nu$.

A qualitative comparison of the non-dimensional quantities can be made between DNS profiles of the dynamic fields and the numerical results from both codes. Variables are expressed in wall units, normalizing with friction velocity u_τ and kinematic viscosity ν. The velocity is nondimensionalized as

$$v^+ = \frac{u}{u_\tau}, . \tag{4}$$

Similarly, the components of the Reynolds stress tensor and the turbulent kinetic energy are normalized as follows

$$\langle u'u' \rangle^+ = \frac{\langle u'u' \rangle}{u_\tau^2}, \; \langle u'v' \rangle^+ = \frac{\langle u'v' \rangle}{u_\tau^2}, \; \langle v'v' \rangle^+ = \frac{\langle v'v' \rangle}{u_\tau^2}, \; k^+ = \frac{k}{u_\tau^2}. \tag{5}$$

All the variables are reported against the non-dimensional radial coordinates

$$x^+ = \frac{r u_\tau}{\nu} . \tag{6}$$

In Figure 3, the non-dimensional velocity profile is displayed on the left and the turbulent kinetic energy on the right. Results from FEMuS and OpenFOAM are labeled in red and blue, respectively. DNS profiles corresponding to the nearest lower and higher Re_τ cases ($Re_\tau = 360$ and $Re_\tau = 550$) are included for reference [12].

The dimensionless velocity and turbulent kinetic energy profiles show very good agreement for FEMuS. For k^+, FEMuS overestimates the near-wall peak across all Re_τ cases. In contrast, OpenFOAM predicts a slightly different velocity profile, which likely contributes to the

discrepancy in u_τ, and significantly underestimates the near-wall peak of the turbulent kinetic energy, showing notable deviations from DNS data.

Overall, these results confirm that FEMuS, which includes explicit formulations for Reynolds stress tensor components and a refined near-wall treatment, can accurately predict liquid-metal turbulent flows. Consequently, FEMuS is adopted to solve the fluid domain in the conjugate heat transfer problem discussed in the next section, while OpenFOAM is used for the solid domain.

4 CONJUGATE HEAT TRANSFER APPLICATION

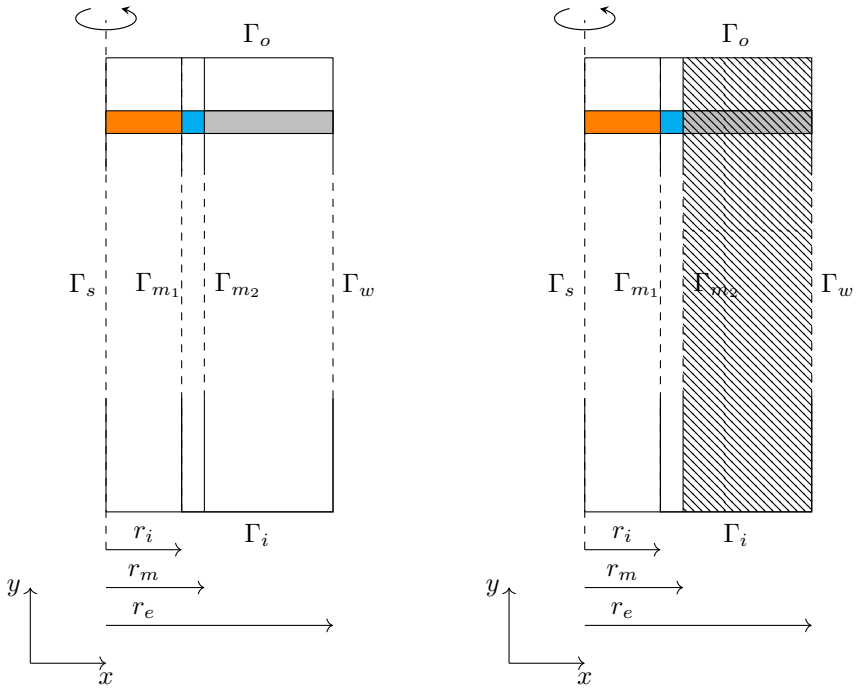

Figure 4: Schematic representation of the computational domains used for the CHT simulations, *Case A* on the left and *Case B* on the right. *Case A* includes the liquid metal domain (orange), the EUROFER pipe domain (blue), and the copper fins domain (gray). *Case B* additionally includes the air domain (black pattern).

In this setup, the entire heat exchanger is simulated using the boundary coupling application, with FEMuS solving the liquid-metal flow and OpenFOAM handling the solid regions. Figure 4 shows the computational domains for the two simulated cases, *Case A* and *Case B*. In both configurations, the orange region represents the PbLi domain, the blue region corresponds to the EUROFER pipe, and the gray region denotes the fins. In the right-hand case, the patterned region indicates the air domain, which fully overlaps the fins region.

The geometry features two distinct interfaces. The first, Γ_{m_1}, couples FEMuS and OpenFOAM, representing the interface between the fluid domain (PbLi flow) and the solid pipe wall. The second, Γ_{m_2}, lies between the two solid regions, specifically connecting the EUROFER pipe to the fins. For both cases, data transfer across Γ_{m_1} is managed by the coupling application described in [11]. Within the conjugate heat transfer framework, FEMuS computes the wall heat flux on Γ_{m_1} and transfers it to OpenFOAM, where it is applied as a non-homogeneous Neumann boundary condition on the inner pipe wall. OpenFOAM, in turn, computes the wall

temperature and returns it to FEMuS as a non-homogeneous Dirichlet boundary condition for the temperature equation. The simulation of the solid domain and the treatment of the Γ_{m_2} interface, instead, are handled differently in *Case A* and *Case B*.

4.1 Case A results

In the first approach, the coupling application is used not only to connect FEMuS and OpenFOAM across Γ_{m_1} but also to couple the two solid regions within OpenFOAM across Γ_{m_2}. At this interface, the heat flux from the EUROFER pipe is applied as a non-homogeneous Neumann boundary condition on the copper fins, while the fins return their wall temperature as a Dirichlet boundary condition to the pipe. This configuration, referred to as *Case A*, is schematically illustrated in Figure 5.

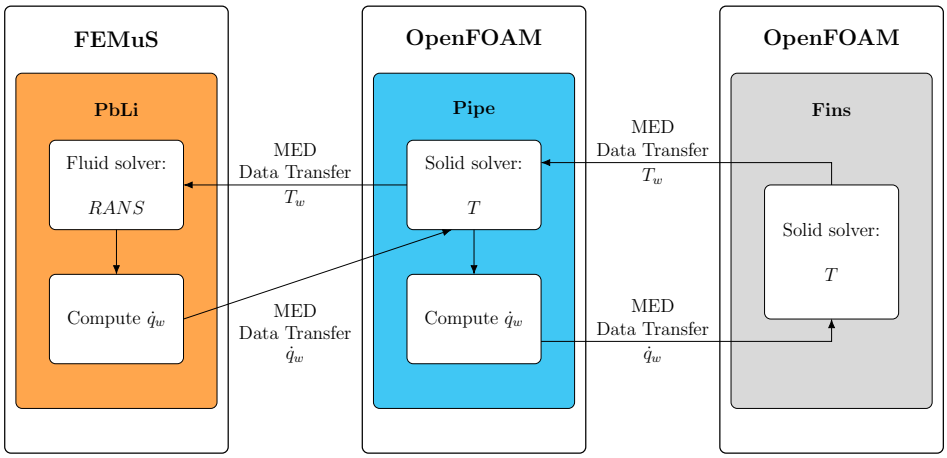

Figure 5: Schematic representation of the coupling algorithm for *Case A*.

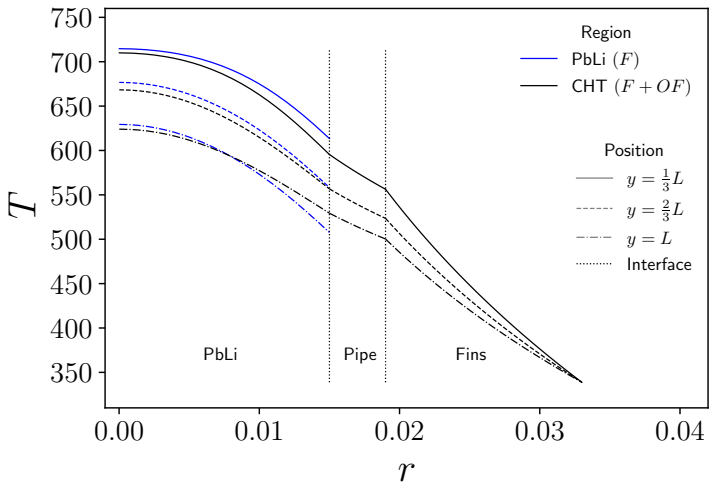

Figure 6: Multi-region radial temperature profiles at three sections of the pipe, $y/L = 1/3$ (solid), $y/L = 2/3$ (dashed) and $y/L = 1$ (dash-dotted), for both the CHT simulation (black) and PbLi flow simulation (blue).

Figure 6 presents the temperature profiles at three different positions along the heat exchanger. The solid line corresponds to $1/3$ of the total pipe length, the dashed profile is taken at $2/3L$, and the remaining profile represents the outlet section of the pipe. The black curves show the radial temperature profiles across the liquid metal, pipe, and fins obtained from the CHT simulation. For comparison, the blue curves represent the results of the standalone FEMuS simulation of the fluid flow temperature as described in the previous section, referred to as PbLi (F). In the PbLi simulation, a constant wall heat flux is applied on the external surface of the fluid domain, Γ_{m_1}, whereas in the CHT simulation, the heat flux on the same surface is spatially non-uniform. This difference leads to non-uniform cooling along the pipe. Near the inlet, the temperature difference between the PbLi and the pipe wall is highest, resulting in the largest wall heat flux. As the flow advances downstream, the temperature difference gradually decreases, leading to a progressive reduction in wall heat flux along the pipe length.

Table 2: Comparison between CHT results with the predicted quantities for *Case A*.

	CHT	Prediction
$T_{b,out}\ [K]$	572.1	573
$T_w\ [K]$	585.8	-
$T_b\ [K]$	633.6	648
$R_{PbLi}\ [K/W]$	0.0028	0.0031
$h\ [W/(m^2K)]$	6413	5704
Nu	8.79	7.81

Table 2 summarizes the computed results and compares them with the predicted values. The bulk temperature at the pipe outlet meets the design requirement, reaching $572.1\,\mathrm{K}$, which is slightly below the target value of $573\,\mathrm{K}$. This corresponds to a total cooling power of $17{,}964\,\mathrm{W}$. The CFD simulation also yields a heat transfer coefficient of $6413\,\mathrm{W/m^2K}$, exceeding the predicted value. This indicates that the convective resistance of the liquid metal flow is lower than initially estimated, leading to a higher simulated Nusselt number than the design prediction.

4.2 Case B results

The second CHT simulation uses the full configuration, which includes the air domain. Unlike the boundary-data transfer approach of *Case A*, this setup employs a dedicated wrapper developed for the OpenFOAM multi-region solver [11]. The Γ_{m_1} interface is handled through the MED library, enabling communication between FEMuS and the OpenFOAM multi-region application. In this configuration, the Γ_{m_2} interface, between the EUROFER pipe and the copper fins, is resolved internally by the OpenFOAM CHT solver, eliminating the need for external coupling. Furthermore, the interaction between the fins and the air domain is modeled using OpenFOAM's `fvModel` functionality, which applies volumetric coupling across the two regions. The overall configuration for *Case B* is schematically illustrated in Figure 7.

Similar considerations to those discussed for *Case A* can be made by examining the radial temperature profiles in Figure 8, evaluated at the same three heights along the pipe. The temperature profile of the liquid metal is shown in blue, the EUROFER pipe and fins in black, and the air domain in red.

Table 3 summarizes the key results and compares them with the predicted values. The CHT

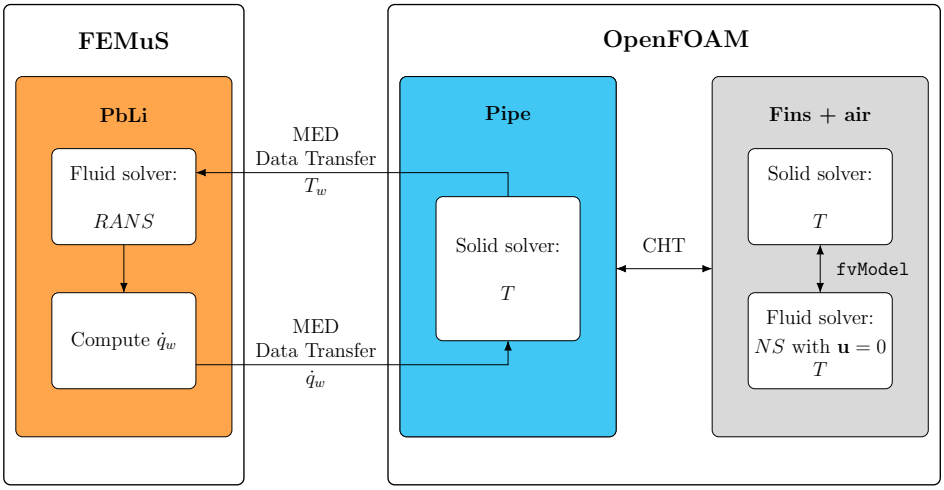

Figure 7: Schematic representation of the coupling algorithm for *Case B*.

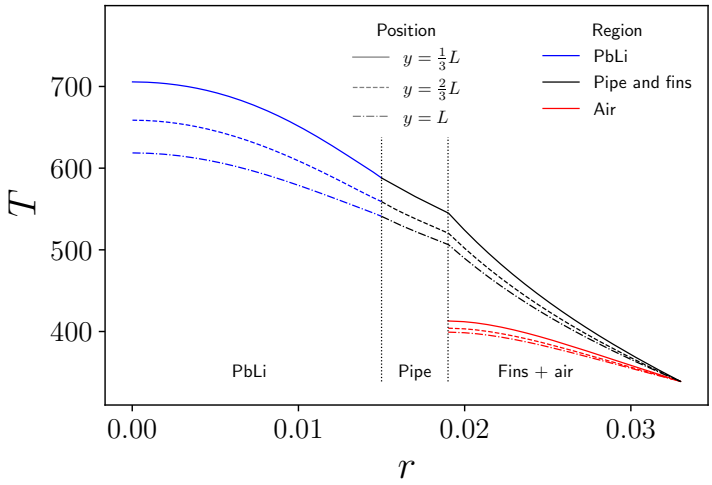

Figure 8: Multi-region radial temperature profiles at three sections of the pipe, $y/L = 1/3$ (solid), $y/L = 2/3$ (dashed) and $y/L = 1$ (dash-dotted), for liquid metal (blue), pipe and fins (black) and air (red).

Table 3: Comparison between CHT results with the predicted quantities for *Case B*.

	CHT	Prediction
$T_{b,out}\ [K]$	571.4	573
$\dot{Q}\ [W]$	18065	17870
$T_w\ [K]$	579.1	-
$T_b\ [K]$	634.1	648
$R_{PbLi}\ [K/W]$	0.0030	0.0031
$h\ [W/(m^2K)]$	5810	5704
Nu	7.97	7.81

simulation yields a Nusselt number of 7.97, slightly higher than the predicted 7.81, indicating

that the convective heat transfer of the liquid metal is marginally more effective than initially estimated.

The results from *Case A* and *Case B* suggest that the theoretical prediction of the Nusselt number may be underestimated, implying a higher actual heat flux. This enhanced heat transfer performance enables the heat exchanger to meet the required outlet temperature while maintaining a sufficient margin above the critical temperature. This safety margin helps account for potential deviations between the computational model and the real system. Additionally, the presence of a reheater downstream of the PbLi heat exchanger further guarantees that the critical temperature threshold is not reached under normal operating conditions.

5 CONCLUSIONS

A realistic liquid-metal heat exchanger with a Lead–Lithium alloy flowing through a finned cylindrical pipe has been analyzed using separate CFD codes for the fluid and solid domains. First, the liquid-metal turbulence has been modeled with FEMuS (anisotropic four-parameter model) and OpenFOAM (`kOmegaSST`), with FEMuS showing better agreement with DNS data in forced turbulent regimes. Two conjugate heat transfer configurations have been investigated within the numerical coupling framework. In the first, the developed MED-based coupling thermally linked the liquid metal, EUROFER pipe, and copper fins. In the second, FEMuS and OpenFOAM were coupled only across the fluid–pipe interface, while OpenFOAM's native multi-region solver handled the pipe–fins interaction internally.

This interface-coupling approach enabled the analysis of liquid-metal heat transfer under non-uniform wall heat flux, yielding a more accurate estimation of convective resistance and Nusselt number compared to predictions. The developed coupling tool proved effective for simulating multiphysics problems beyond the capabilities of stand-alone commercial codes and can be extended to additional solvers and physical models for future applications.

REFERENCES

[1] H. Jasak, A. Jemcov, and Z. Tukovic, *OpenFOAM: A C++ library for complex physics simulations*, in *International Workshop on Coupled Methods in Numerical Dynamics*, Vol. 1000, pp. 1–20, September 2007.

[2] G. Barbi, A. Cervone, F. Giangolini, S. Manservisi, and L. Sirotti, *Numerical Coupling between a FEM Code and the FVM Code OpenFOAM Using the MED Library*, *Applied Sciences*, vol. 14, no. 9, p. 3744, 2024.

[3] G. Barbi, G. Bornia, D. Cerroni, A. Cervone, A. Chierici, L. Chirco, ..., and R. Scardovelli, *FEMuS-Platform: A numerical platform for multiscale and multiphysics code coupling*, in *9th International Conference on Computational Methods for Coupled Problems in Science and Engineering, COUPLED PROBLEMS 2021*, pp. 1–12, International Center for Numerical Methods in Engineering, 2021.

[4] A. Ribes and C. Caremoli, *Salome platform component model for numerical simulation*, in *31st Annual International Computer Software and Applications Conference (COMPSAC 2007)*, vol. 2, pp. 553–564, IEEE, July 2007.

[5] A. Ying, M. Abdou, C. Wong, S. Malang, N. Morley, M. Sawan, ..., and S. Zinkle, *An overview of US ITER test blanket module program*, *Fusion Engineering and Design*, vol. 81, no. 1–7, pp. 433–441, 2006.

[6] C. Ciurluini, V. Narcisi, A. Tincani, C. O. Ferrer, and F. Giannetti, *Conceptual design overview of the ITER WCLL Water Cooling System and supporting thermal-hydraulic analysis*, *Fusion Engineering and Design*, vol. 171, p. 112598, 2021.

[7] D. Martelli, A. Venturini, and M. Utili, *Literature review of lead-lithium thermophysical properties*, *Fusion Engineering and Design*, vol. 138, pp. 183–195, 2019.

[8] K. Mergia and N. Boukos, *Structural, thermal, electrical and magnetic properties of Eurofer 97 steel*, *Journal of Nuclear Materials*, vol. 373, no. 1–3, pp. 1–8, 2008.

[9] H. Hattori, A. Morita, and Y. Nagano, *Nonlinear eddy diffusivity models reflecting buoyancy effect for wall-shear flows and heat transfer*, *International Journal of Heat and Fluid Flow*, vol. 27, no. 4, pp. 671–683, 2006.

[10] G. Barbi, V. Giovacchini, and S. Manservisi, *A New Anisotropic Four-Parameter Turbulence Model for Low Prandtl Number Fluids*, *Fluids*, vol. 7, no. 1, p. 6, 2021.

[11] L. Sirotti, *Development of a CFD tool for turbulent natural convection and heat transfer simulations of liquid metals*, Ph.D. thesis, Alma Mater Studiorum – Università di Bologna, June 2025.

[12] G. K. El Khoury, P. Schlatter, A. Noorani, P. F. Fischer, G. Brethouwer, and A. V. Johansson, *Direct numerical simulation of turbulent pipe flow at moderately high Reynolds numbers*, *Flow, Turbulence and Combustion*, vol. 91, no. 3, pp. 475–495, 2013.